AIAA 81-0260R

A Theoretical and Experimental Investigation of the Constant Area, Supersonic-Supersonic Ejector

J. C. Dutton*
Texas A&M University, College Station, Texas
C. D. Mikkelsen†
U.S. Army Missile Command, Redstone Arsenal, Alabama
and
A. L. Addy‡
University of Illinois at Urbana-Champaign, Urbana, Illinois

An investigation of the constant area, supersonic-supersonic ejector has been conducted wherein one supersonic stream is pumped directly by another inside a confining duct. The theoretical analysis is based on simplified, one-dimensional models of the constant area mixing section and inviscid interaction region. The parametric dependence of the ejector pressure recovery performance on each of seven dimensionless variables is presented. A series of small-scale, axisymmetric ejector experiments indicates that the theory predicts maximum ejector compression ratios that are 15-22% higher than the measured values and that the ejector is susceptible to separation of the secondary stream at the point of confluence of the primary and secondary streams.

Nomenclature

A	= area
B	= quantity defined in Eq. (8)
D	= diameter
f_1,f_2,f_3,f_4	= functions of γ and M defined by Eqs. (2), (4), (9), and (14), respectively
M	= Mach number
MW	= molecular weight
P	= pressure
Re	= Reynolds number
T	= temperature
V	= velocity
W	= mass flow rate
γ	= specific heat ratio
μ	= absolute viscosity
ρ	= density

Subscripts and Superscripts

lim	= limiting condition
M	= mixed
P	= primary
S	= secondary
T	= throat
0	= stagnation
$1,2,3$	= station 1, 2, or 3 in Fig. 2
*	= sonic condition

Introduction

SUPERSONIC ejector-diffuser systems have many applications as both pressure recovery and thrust augmentation devices. However, the application that provides the primary motivation for this work is the high-energy chemical laser. In the continuous-wave chemical laser, alternate, interleaved streams of fuel (H_2 or D_2) and oxidant (F) enter the laser cavity at high Mach numbers and a low static pressure. These streams then mix and react to establish the lasing zones between the streams. Accompanying the chemical reactions, a significant quantity of heat is released to the laser flow which tends qualitatively to increase the static pressure, decrease the stagnation pressure, and decrease the Mach number of the "mixed" supersonic laser flow. At the laser cavity exit, the flow is hot ($T_0 \simeq 1500$ K), highly corrosive, supersonic ($1.5 < M < 2.5$), and at low static pressure ($1 < P < 10$ kPa). This stream must then be pumped to ambient conditions so that the lasing process can be started and sustained.

The conventional approach to the pressure recovery problem, Fig. 1a, has been first to diffuse the laser flow using a constant area supersonic diffuser followed by a subsonic diffuser and then to pump the resulting subsonic flow with a supersonic ejector. The mixing tube of this subsonic-supersonic ejector is then generally followed by a second subsonic diffuser. An alternate approach to the problem is the supersonic-supersonic ejector, Fig. 1b. In this system, the diffusers located between the cavity exit and the ejector are eliminated, and the supersonic laser cavity flow is pumped directly with a supersonic ejector. This concept offers the advantage of reducing the overall device length, with a possible increase in performance. Since the physical size of the combined laser/pumping system is dominated by the pressure recovery equipment, this approach may also result in a substantial weight and volume reduction for the system. The objective of the present paper is to present the results of an integrated theoretical and experimental investigation of the supersonic-supersonic ejector.

Previous Work

The topic of ejectors has been extensively studied over the years, as evidenced by Mikkelsen's compilation[1] of over 350 references concerning ejector systems and related topics. Most of these publications, however, were concerned with pumping a subsonic, or even stagnant, secondary stream; this is not surprising when one considers the wide variety of industrial applications for such devices.

Presented as Paper 81-0260 at the AIAA 19th Aerospace Sciences Meeting, St. Louis, Mo., Jan. 12-15, 1981; submitted March 14, 1981; revision received Feb. 16, 1982.

*Assistant Professor, Dept. of Mechanical Engineering. Member AIAA.
†Aerospace Engineer. Member AIAA.
‡Professor and Associate Head, Dept. of Mechanical and Industrial Engineering. Associate Fellow AIAA.

The earliest work concerned with ejector pumping of supersonic streams appears to be that of Spiegel et al.,[2] which was reported in 1953. This was the first of four NACA reports[2-5] concerned with the possibility of using supersonic air injection to reduce the required starting and running pressure ratios of supersonic and hypersonic wind tunnels. Both Spiegel et al.[2] and Hunczak and Rousso[3] performed one-dimensional analyses of the tunnel circuit including auxiliary supersonic air injection just downstream of the test section. Experiments were also performed that demonstrated that reduced pressure ratios were obtained with supersonic injection, although the pressure recovery was not as favorable as that obtained from variable-geometry, second-throat-diffuser tunnels. Hasel and Sinclair[4] experimentally investigated the possibility of using supersonic injection in conjunction with a variable-geometry diffuser for increasing the pressure recovery of supersonic wind tunnels. They found that the injection enhanced the tunnel pressure recovery, particularly for the higher test section Mach numbers that were considered, $3 \leq M \leq 5$. Stokes[5] also reported use of supersonic air injection together with a variable-geometry diffuser in a hypersonic tunnel. Unfortunately, no pressure recovery data were reported.

As mentioned in the Introduction, the recent development of the chemical laser has spawned renewed interest in the supersonic-supersonic ejector as a means of pumping the supersonic laser cavity flow directly. Zimet[6] performed an experimental study of the steady state and transient operation of a supersonic ejector with both subsonic and supersonic secondary flow. It was concluded that the supersonic-supersonic mode showed good potential for weight-volume reductions at increased performance, but that starting problems were more critical than for the conventional subsonic-supersonic configuration. Batt and Behrens[7] also obtained experimental data on a supersonic-supersonic ejector configuration that was somewhat different from the one investigated herein. A strut-mounted primary supply nozzle that required wall contour expansion for optimal performance was submerged in the supersonic secondary stream. Both cold airflow tests and one hot fire, laser demonstration test were performed. The hot fire experiment demonstrated above-atmospheric pressure recovery and sea-level atmospheric start at the design point flow condition.

Theory

There are several methods available to analyze the pumping performance of the supersonic-supersonic ejector; these include one-dimensional analysis, the method of integral relations, the method of characteristics, and finite difference techniques. For the latter methods the flowfield may be described in increasing detail, but the computer time necessary both to develop the appropriate programs and to calculate individual cases increases proportionately. Since the purpose of the present study is to develop a simplified, general theory for the pressure recovery performance of the supersonic-supersonic ejector and to investigate parametrically the feasibility of utilizing this device to pump laser cavity flow, a one-dimensional approach has been adopted. As such, the method is computationally simple and is well-suited to parametric studies and optimization procedures although it provides little insight into the details of the actual flowfield.

The analysis is similar to that performed by Fabri et al.[8,9] for the subsonic-supersonic ejector. The conservation equations are applied to an overall control volume contained within the constant area ejector mixing tube assuming uniform velocity and pressure distributions for the primary and secondary streams at the tube entrance and a fully mixed, uniform stream at the exit. These relations allow determination of the exit conditions, but it is well known[4,8-11] that all arbitrary combinations of inlet conditions are not possible. In particular, as the static pressure of the primary stream at the mixing tube inlet is increased above that of the secondary, a condition is eventually reached for which the secondary stream is compressed to sonic conditions at the "aerodynamic throat" formed just downstream of the tube inlet. A second set of control volume relations is used to predict the operation of the ejector at this "upper limit point."

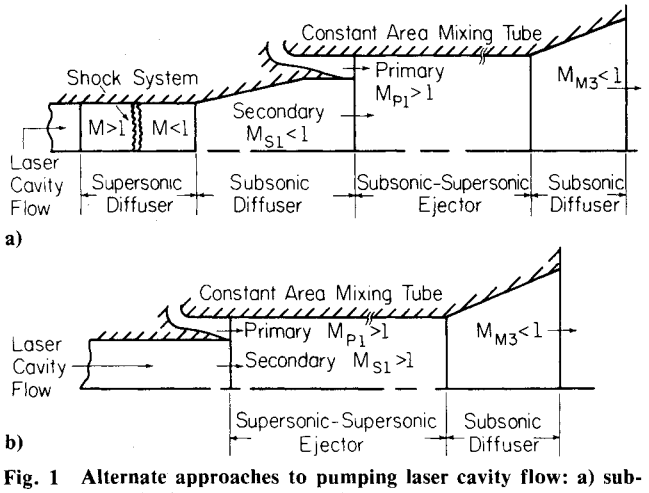

Fig. 1 Alternate approaches to pumping laser cavity flow: a) subsonic-supersonic ejector; b) supersonic-supersonic ejector.

Overall Control Volume Analysis

The continuity, momentum, and energy conservation equations are applied[1,12] to a control volume spanning the mixing tube from inlet to exit, stations 1 to 3 in Fig. 2. Assuming the steady, frictionless, adiabatic flow of an ideal gas with constant specific heats, the conditions at the tube exit can be determined upon specification of the following eight parameters: the inlet Mach numbers of the primary and secondary streams, M_{PI} and M_{SI}; the specific heat ratios, γ_P and γ_S; the stagnation temperature and molecular weight ratios, T_{0P}/T_{0S} and MW_P/MW_S; and the inlet stagnation pressure and area ratios of the primary-to-secondary streams, P_{0PI}/P_{0SI} and A_{PI}/A_{SI}.

The stagnation pressure ratio at the inlet is first transformed to the equivalent static pressure ratio by using the isentropic flow function,

$$\frac{P_{PI}}{P_{SI}} = \frac{P_{0PI}}{P_{0SI}} \frac{f_1(\gamma_S, M_{SI})}{f_1(\gamma_P, M_{PI})} \tag{1}$$

where

$$f_1(\gamma, M) \equiv \left(1 + \frac{\gamma - 1}{2} M^2\right)^{\gamma/(\gamma-1)} \tag{2}$$

The primary-to-secondary mass flow ratio can then be determined from the mass flow function as

$$\frac{W_P}{W_S} = \frac{P_{PI}}{P_{SI}} \frac{A_{PI}}{A_{SI}} \left[\frac{MW_P}{MW_S} \frac{T_{0S}}{T_{0P}}\right]^{1/2} \frac{f_2(\gamma_P, M_{PI})}{f_2(\gamma_S, M_{SI})} \tag{3}$$

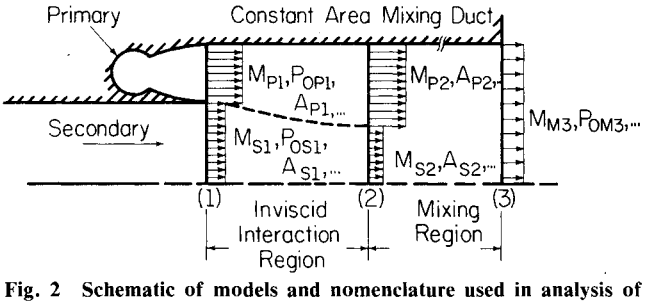

Fig. 2 Schematic of models and nomenclature used in analysis of constant area, supersonic-supersonic ejector.

where

$$f_2(\gamma,M) \equiv M\left[\gamma\left(1+\frac{\gamma-1}{2}M^2\right)\right]^{1/2} \tag{4}$$

With this information, the specific heat ratio and molecular weight ratio of the fully mixed exit flow are found from

$$\gamma_M = \gamma_S\left\{\left[1+\frac{W_P}{W_S}\frac{\gamma_P}{\gamma_S}\frac{(\gamma_S-1)}{(\gamma_P-1)}\frac{\mathrm{MW}_S}{\mathrm{MW}_P}\right]\Big/\left[1+\frac{W_P}{W_S}\frac{(\gamma_S-1)}{(\gamma_P-1)}\frac{\mathrm{MW}_S}{\mathrm{MW}_P}\right]\right\} \tag{5}$$

$$\mathrm{MW}_M/\mathrm{MW}_S = \left(1+\frac{W_P}{W_S}\right)\Big/\left(1+\frac{W_P}{W_S}\frac{\mathrm{MW}_S}{\mathrm{MW}_P}\right) \tag{6}$$

Likewise, the stagnation temperature ratio of the mixed flow can be determined from the energy and continuity equations as

$$T_{0M}/T_{0S} = \left[1+\frac{W_P}{W_S}\frac{\gamma_P}{\gamma_S}\frac{(\gamma_S-1)}{(\gamma_P-1)}\frac{\mathrm{MW}_S}{\mathrm{MW}_P}\frac{T_{0P}}{T_{0S}}\right]\Big/\left[1+\frac{W_P}{W_S}\frac{\gamma_P}{\gamma_S}\frac{(\gamma_S-1)}{(\gamma_P-1)}\frac{\mathrm{MW}_S}{\mathrm{MW}_P}\right] \tag{7}$$

By combining the continuity and momentum equations written for the overall control volume, the exit Mach number and pressure ratios can be calculated using

$$B \equiv \left\{\left(1+\frac{W_P}{W_S}\right)f_2(\gamma_S,M_{S1})\left[\frac{T_{0M}}{T_{0S}}\frac{\mathrm{MW}_S}{\mathrm{MW}_M}\right]^{1/2}\right\}\Big/\left\{f_3(\gamma_S,M_{S1})+\frac{P_{P1}}{P_{S1}}\frac{A_{P1}}{A_{S1}}f_3(\gamma_P,M_{P1})\right\} \tag{8}$$

where

$$f_3(\gamma,M) \equiv 1+\gamma M^2 \tag{9}$$

and

$$M_{M3}^2 = \frac{\gamma_M(1-2B^2)\pm(\gamma_M^2-2B^2\gamma_M^2-2B^2\gamma_M)^{1/2}}{2B^2\gamma_M^2-\gamma_M^2+\gamma_M} \tag{10}$$

$$\frac{P_{M3}}{P_{S1}} = \left[f_3(\gamma_S,M_{S1})+\frac{P_{P1}}{P_{S1}}\frac{A_{P1}}{A_{S1}}f_3(\gamma_P,M_{P1})\right]\Big/\left[f_3(\gamma_M,M_{M3})\left(1+\frac{A_{P1}}{A_{S1}}\right)\right] \tag{11}$$

$$\frac{P_{0M3}}{P_{0S1}} = \frac{P_{M3}}{P_{S1}}\frac{f_1(\gamma_M,M_{M3})}{f_1(\gamma_S,M_{S1})} \tag{12}$$

Note that two roots are indicated for the square of the exit Mach number M_{M3}^2 since it is obtained from the solution of a quadratic equation. The root obtained using the positive sign is a supersonic solution and may be thought of as the uniform supersonic Mach number "equivalent" to the piecewise uniform primary and secondary Mach numbers at the mixing tube entrance. The root obtained with the negative sign is a subsonic solution and is the one utilized here since it is assumed that the mixing tube is sufficiently long that the exit flow is fully mixed and diffused to subsonic conditions. It is interesting to note that, if the supersonic solution is allowed to diffuse through a normal shock wave, the subsonic solution is obtained. This result should not be surprising since the relations developed here are a multistream equivalent of the one-dimensional Fanno-Rayleigh relations for a normal shock wave.

Control Volume Analysis of the Inviscid Interaction Region

If the primary-to-secondary inlet static pressure ratio is greater than unity ($P_{P1}/P_{S1}>1$), the secondary flow is compressed by the mutual interaction of the primary and secondary streams within the mixing tube, Fig. 2. As previously mentioned, this process is limited, in a one-dimensional sense, to a compression of the secondary stream to sonic flow conditions at the aerodynamic throat formed just downstream from the mixing tube inlet. This limiting condition is analyzed by writing integral conservation relations for control volumes which extend from the tube entrance to the aerodynamic throat location, stations 1 to 2 in Fig. 2. It is assumed that the streams remain distinct and do not mix in this initial interaction region and that the flow for each stream is isentropic between stations 1 and 2. These assumptions, together with the facts that the mixing tube area is constant and that the secondary Mach number at the aerodynamic throat is unity, $M_{S2}=1$, allow determination of this limiting operating condition. One consequence of this model is that the *average*, one-dimensional static pressures of the streams can be different at a given axial location. Of course, the true, two-dimensional boundary conditions across the slipline between the streams are equality of static pressure and flow direction.

By writing continuity equations for each individual stream and a momentum equation for the combination of the two, the limiting point of operation can be determined from the following computations. First the primary Mach number at the choking location, M_{P2}, is found as the supersonic solution of the following implicit relation,

$$f_4(\gamma_P,M_{P2}) = f_4(\gamma_P,M_{P1})\left[1+\frac{f_4(\gamma_S,M_{S1})-1}{(A_{P1}/A_{S1})f_4(\gamma_S,M_{S1})}\right] \tag{13}$$

where the function f_4 is the isentropic area ratio function, A/A^*,

$$f_4(\gamma,M) = \frac{A}{A^*}(\gamma,M) \equiv \frac{1}{M}\left[\left(\frac{2}{\gamma+1}\right)\left(1+\frac{\gamma-1}{2}M^2\right)\right]^{(\gamma+1)/2(\gamma-1)} \tag{14}$$

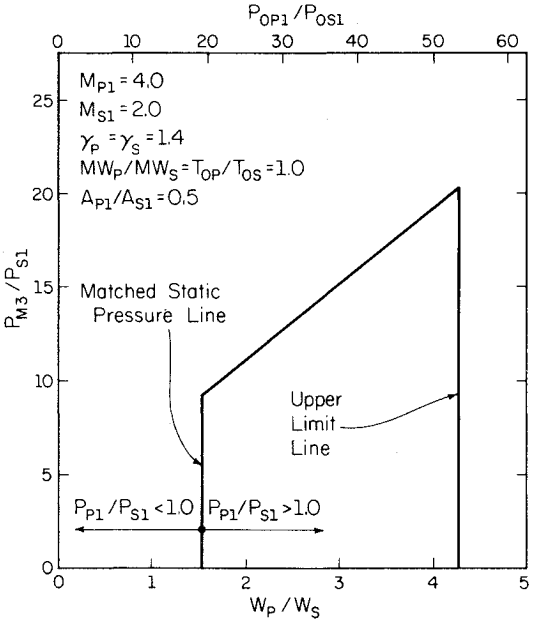

Fig. 3 Operating plane for baseline case of constant area, supersonic-supersonic ejector.

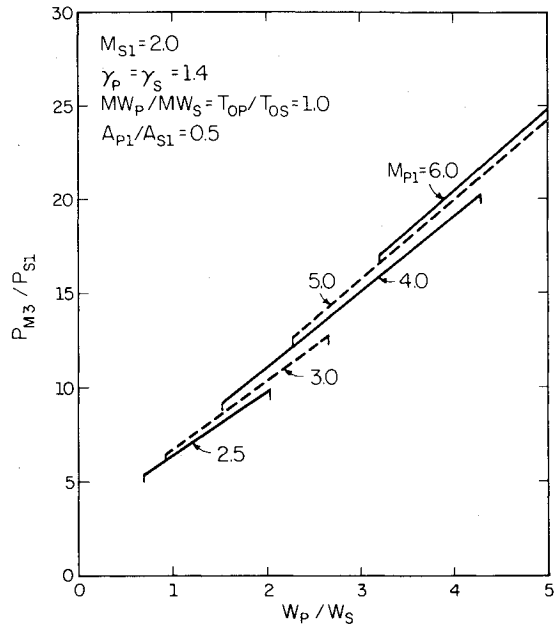

Fig. 4 Parametric effect of M_{PI} on ejector pressure recovery.

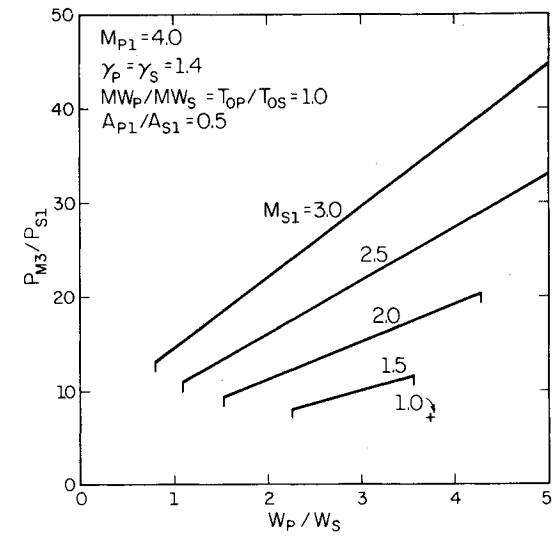

Fig. 5 Parametric effect of M_{SI} on ejector pressure recovery.

With M_{P2} determined, the primary-to-secondary inlet static pressure ratio at the limit condition can be calculated from

$$\left(\frac{P_{PI}}{P_{SI}}\right)_{\text{lim}} = [f_3(\gamma_S, M_{SI}) - f_2(\gamma_S, M_{SI}) f_3(\gamma_S, 1)/f_2(\gamma_S, 1)]/$$

$$(A_{PI}/A_{SI})\,[f_2(\gamma_P, M_{PI}) f_3(\gamma_P, M_{P2})/f_2(\gamma_P, M_{P2})$$

$$- f_3(\gamma_P, M_{PI})] \qquad (15)$$

A given operating point satisfies the aerodynamic compression criterion for started supersonic secondary flow if $(P_{PI}/P_{SI}) \leq (P_{PI}/P_{SI})_{\text{lim}}$.

If the primary static pressure at the inlet is *less* than that of the secondary, $P_{PI}/P_{SI} < 1$, this limit condition analysis can be repeated where compression of the primary stream to sonic conditions is now of concern. For operating points near the point of maximum ejector pressure recovery, however, the condition $P_{PI}/P_{SI} > 1$ prevails. Further details concerning the theoretical analysis may be found in Refs. 1 and 12.

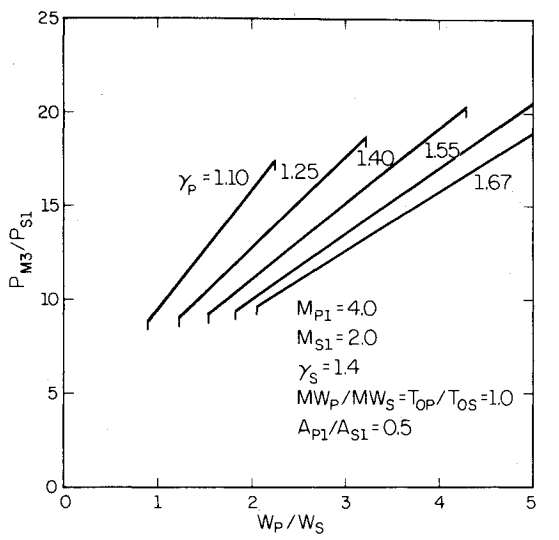

Fig. 6 Parametric effect of γ_P on ejector pressure recovery.

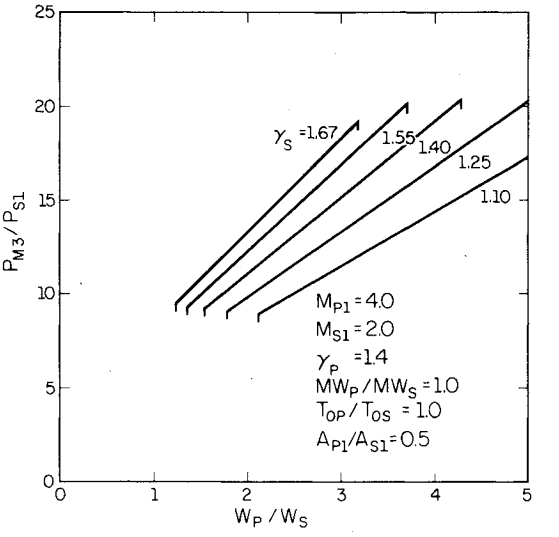

Fig. 7 Parametric effect of γ_S on ejector pressure recovery.

Parametric Study

Utilizing the simplified, one-dimensional analysis described in the preceding sections, it is a straightforward task to perform a parametric study to determine the dependence of the ejector's pressure recovery performance on the dimensionless variables of importance. As previously mentioned, the analysis identifies eight such parameters: M_{PI}, M_{SI}, γ_P, γ_S, T_{0P}/T_{0S}, MW_P/MW_S, A_{PI}/A_{SI}, and P_{0PI}/P_{0SI}. Because of this large number of variables, a rational scheme for conducting the study is needed. The method used is to define a baseline case and then to vary a single parameter at a time about this case. The baseline configuration is defined by $M_{PI}=4.0$, $M_{SI}=2.0$, $\gamma_P=\gamma_S=1.4$, $T_{0P}/T_{0S}=MW_P/MW_S=1.0$, and $A_{PI}/A_{SI}=0.5$. In this study, the primary-to-secondary stagnation pressure ratio at the tube inlet, P_{0PI}/P_{0SI}, is used as the independent variable in obtaining primary-to-secondary mass flow variations so that curves of pressure recovery vs mass flow ratio can be developed.

The ejector operating plane for the baseline case is presented in Fig. 3, where the exit-to-secondary inlet static pressure ratio is plotted as a function of the primary-to-secondary mass flow ratio. The upper line is the series of maximum compression ratio operating points defined by the overall control volume analysis assuming a uniform, fully

mixed, subsonic flow at the exit of the constant area mixing tube. The vertical line at the right is the limiting condition defined in the preceding section by the compression of the secondary stream to sonic conditions at the aerodynamic throat. For larger mass flow ratios, the one-dimensional model of the inviscid interaction region predicts that started supersonic flow of the secondary stream is not possible. The vertical line at the left marks the operating point at which the static pressures of the primary and secondary streams at the mixing tube inlet are equal. As can also be seen in the figure, the maximum ejector compression ratio increases with increasing primary-to-secondary inlet static pressure ratio. It is interesting to note that the relation between the maximum ejector pressure ratio and the mass flow ratio is very nearly linear although the set of equations, (1-12), used to determine it are decidedly nonlinear.

Figures 4-9 present the parametric dependence of the ejector pressure recovery performance on the variables M_{PI}, M_{SI}, γ_P, γ_S, MW_P/MW_S, T_{0P}/T_{0S}, and A_{PI}/A_{SI}. In each case the performance is plotted over the mass flow ratio range from the matched static pressure to upper limit operating points. Although the molecular weight and stagnation temperature ratios are, in general, independent parameters, their effect on the ejector operating plane was identical in this study since only one of these parameters at a time was varied while the other remained at unity. The influence of the MW_P/MW_S and T_{0P}/T_{0S} variations has been combined in Fig. 8.

By inspecting these figures, it is seen that, in terms of increased compression ratios for a given primary-to-secondary mass flow ratio, the ejector pumping performance is only weakly dependent on the inlet primary Mach number, moderately dependent on the specific heat and entrance area ratios, and strongly dependent on the secondary inlet Mach number and the stagnation temperature and molecular weight ratios. From Fig. 5, which presents the parametric dependence on the secondary inlet Mach number, it appears that by expanding the secondary to obtain higher values of M_{SI}, improved pressure recovery is obtained. For a fixed secondary inlet stagnation pressure, however, just the opposite is true: expansion of the secondary leads to a decreased inlet static pressure P_{SI}, which is used as the normalizing pressure on the ordinate of Fig. 5. This, in turn, leads to a reduced exit static pressure P_{M3}. Note that the compression ratio at which the matched static pressure point occurs increases strongly as M_{PI} is increased and is only moderately or weakly dependent on the other six parameters. This observation is important since the experiments indicate that, as the inlet primary static

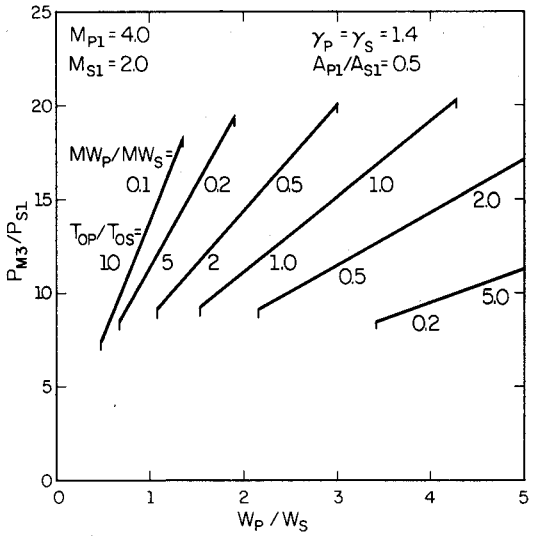

Fig. 8 Parametric effects of MW_P/MW_S and T_{0p}/T_{0S} on ejector pressure recovery.

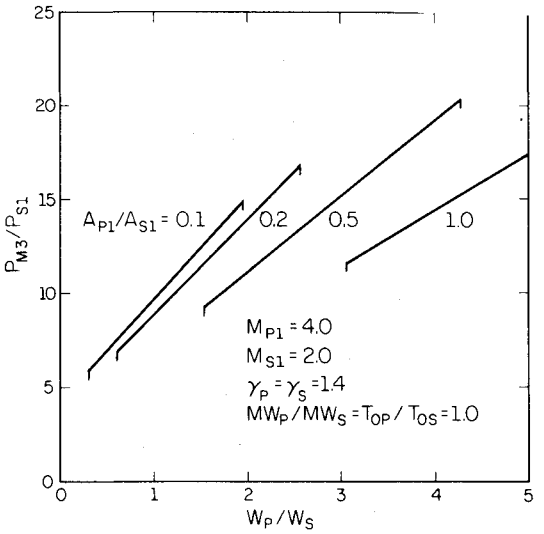

Fig. 9 Parametric effect of A_{PI}/A_{SI} on ejector pressure recovery.

pressure is increased above that of the secondary, separation of the secondary stream at the confluence point occurs, with an accompanying degradation in the ejector performance. Therefore, the most effective means for improving ejector pressure recovery are to compress the secondary stream toward sonic conditions, either upstream of the ejector or in the mixing tube, and to operate near the matched static pressure point with a high Mach number, high stagnation temperature, low molecular weight primary gas.

Experiments

A series of small-scale, cold-flow, air-to-air ejector experiments has been conducted both to compare with the previously described theoretical analysis and to obtain a more detailed flowfield description than is provided by the one-dimensional, control volume approach.

Experimental Equipment and Apparatus

A half-section schematic of the axisymmetric, supersonic-supersonic ejector is shown in Fig. 10. The primary flow enters the ejector from a large stagnation chamber at the bottom of the apparatus and is accelerated through the centrally located supersonic primary nozzle. The secondary flow enters the secondary stagnation chamber from two sides and is accelerated through the annular passage formed by the outer wall of the primary nozzle and the mixing tube base. Both the primary and secondary nozzles have elliptical entrance sections and were designed by the method of characteristics to produce uniform distributions of velocity and pressure at their confluence point. The Mach numbers and primary-to-secondary area ratios at the mixing tube entrance for the five ejector configurations tested are given in Table 1.

Static pressure taps were installed along the mixing tube wall, from the nozzle exit plane to the mixing tube exit, at increments of one tube radius. A series of six static wall taps, not shown in Fig. 10, were equally spaced about the mixing tube axis at the nozzle exit plane to check the concentricity of the nozzle and mixing tube. An additional five wall pressure taps, also not shown, were located upstream of the nozzle exit plane at increments of 2.54 mm to ensure that the entering secondary flow was supersonic. It should be noted that in all but one series of experiments the constant area mixing tubes were 10 tube diameters in length.

A final stagnation chamber and back pressure control valve were located downstream from the mixing tube exit. The purpose of the stagnation chamber was to prevent local disturbances at the control valve from influencing the velocity

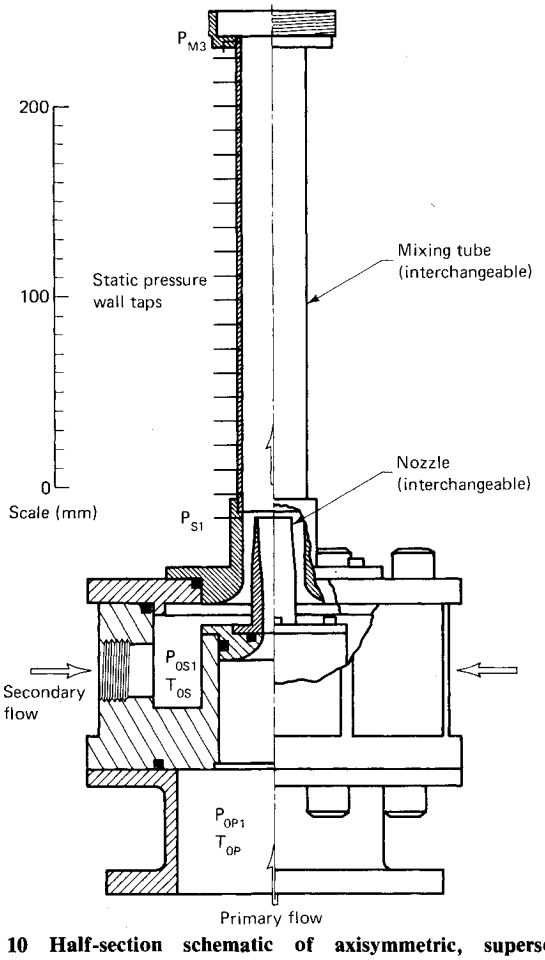

Fig. 10 Half-section schematic of axisymmetric, supersonic-supersonic ejector apparatus.

Table 1 Inlet Mach numbers and area ratios for the supersonic-supersonic ejector experiments

	M_{P1}	M_{S1}	A_{P1}/A_{S1}
1	2.50	1.50	0.51
2	2.50	1.75	0.51
3	2.50	2.00	1.13
4	2.50	2.50	1.13
5	4.00	2.00	1.13

and pressure distributions of the mixed, subsonic flow at the tube exit. For one experiment, a traversing pitot probe was added between the mixing tube and final stagnation chamber for measurement of the exit Mach number distribution.

The experiments were conducted in the Mechanical Engineering Laboratory utilizing both the continuous airflow facility and a specially designed and constructed high-pressure supply system. Mass flow rates for the primary and secondary streams were measured with standard VDI nozzles. Depending on its level, pressure data were recorded with precision Bourdon-tube gages, manometers, or a strain gage transducer-digital counter system. The accuracy of the pressure measurements was approximately within ±1.5 kPa, and the data were repeatable to within approximately ±1%.

Experimental Procedure

Maximum compression ratio data for each experimental ejector configuration were obtained in the following manner. With the back pressure control valve fully open, the secondary stagnation pressure P_{0S1} was set at a fixed value to be maintained by the secondary automatic controller. The automatic controller for the primary stagnation pressure P_{0P1} was then set such that the mass flow ratio W_P/W_S would lie within the operating plane for the ejector configuration being considered. The back pressure valve was then closed until the secondary inlet static pressure P_{S1} began to rise, indicating maximum compression conditions. At this point the mixing

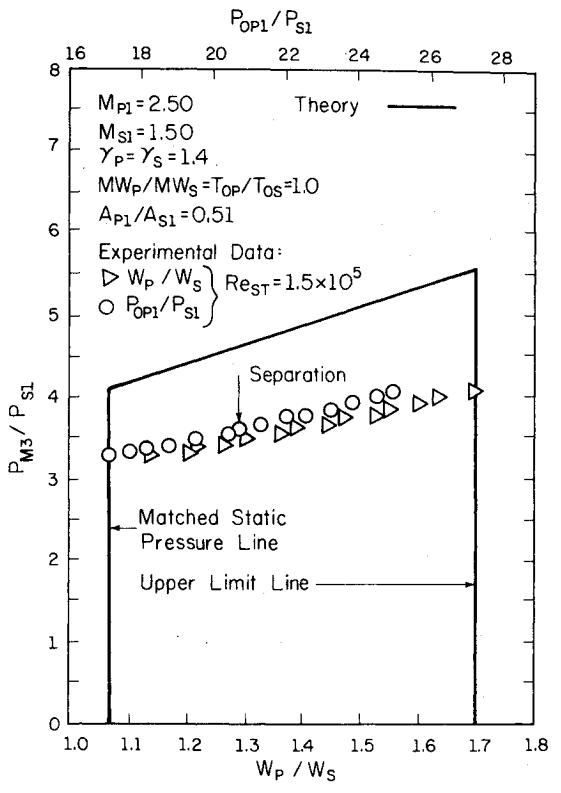

Fig. 11 Comparison of experimental and theoretical ejector compression characteristics, $M_{P1}/M_{S1}=2.5/1.5$.

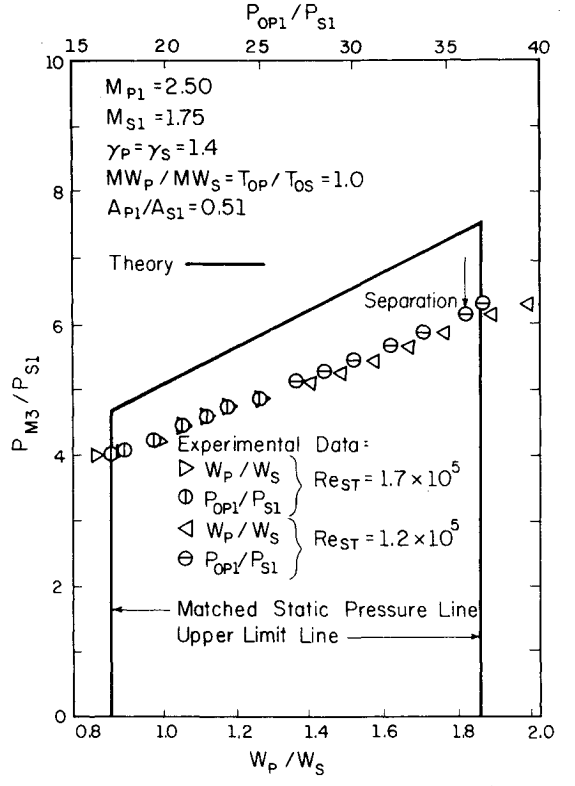

Fig. 12 Comparison of experimental and theoretical ejector compression characteristics, $M_{P1}/M_{S1}=2.5/1.75$.

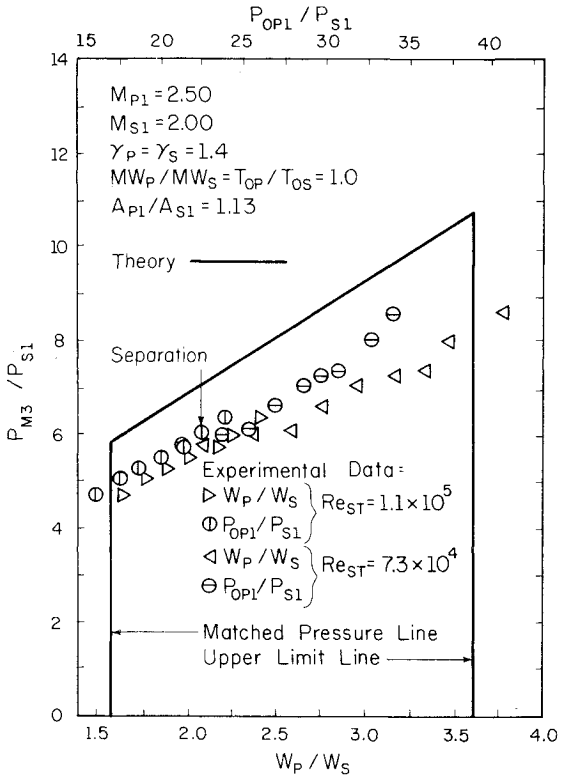

Fig. 13 Comparison of experimental and theoretical ejector compression characteristics, $M_{P1}/M_{S1}=2.5/2.0$.

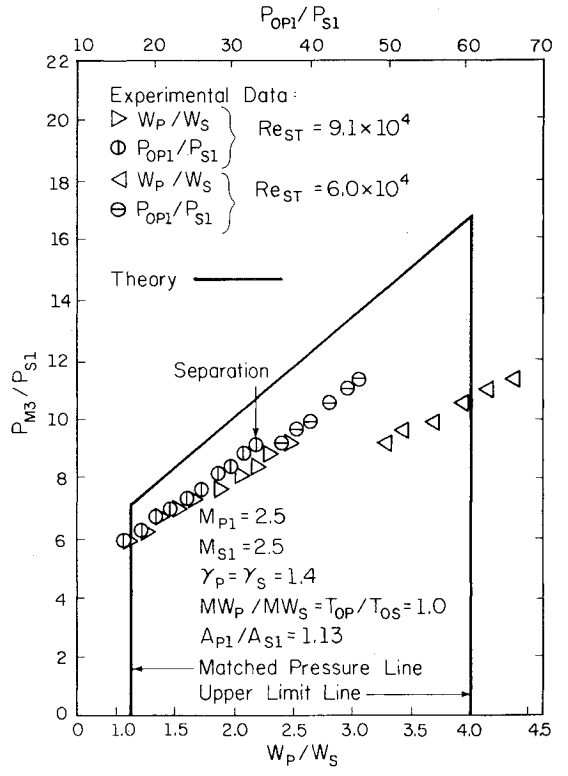

Fig. 14 Comparison of experimental and theoretical ejector compression characteristics, $M_{P1}/M_{S1}=2.5/2.5$.

tube axial-wall pressure distribution and exit pressure were recorded. This process was repeated for various combinations of P_{0S1} and P_{0P1} until the entire mass flow ratio range was covered, unless otherwise restricted by the facility supply pressure. Reference 1 can be consulted for additional information regarding the experimental equipment and procedure.

Results and Discussion

The maximum compression characteristics for the experimental, constant area, supersonic-supersonic ejector configurations listed in Table 1 are presented in Figs. 11-15. For each ejector configuration investigated, the compression ratio data were recorded at one or two secondary nozzle throat Reynolds numbers,

$$Re_{ST}=(\rho V/\mu)\,(D_{M3}-D_S^*) \tag{16}$$

where ρ, V, and μ are the density, velocity, and absolute viscosity, respectively, of the secondary stream evaluated at the throat, and $(D_{M3}-D_S^*)$ is the difference between the outer and inner diameters at the throat. In addition, at each operating point the pressure ratio was determined and plotted against two independent variables: 1) the mass flow ratio W_P/W_S as determined from the VDI nozzle measurements and 2) the primary stagnation-to-secondary static pressure ratio at the inlet, P_{0P1}/P_{S1}. These two points should exactly coincide since W_P/W_S is theoretically proportional to P_{0P1}/P_{S1}. However, by examining the figures it can be seen that the VDI measurements yield W_P/W_S values that are 0-44% greater than the P_{0P1}/P_{S1} values. In addition, it was found that the magnitude of the disagreement increases as the secondary Reynolds number decreases and as W_P/W_S (and, therefore, P_{P1}/P_{S1}) increases. These observations are strong evidence that the boundary layer of the secondary stream may separate at the primary/secondary confluence point. Referring to Fig. 2, it is seen that for $P_{P1}/P_{S1}>1$ the secondary boundary layer approaching the confluence point must negotiate a compression (adverse pressure gradient) with the associated change in direction. For strong adverse pressure gradients, the boundary layer will separate somewhere upstream, so that the secondary stream will not be "flowing full" at the mixing tube inlet. For this condition, values of W_P/W_S based on the geometrical area A_{S1} and the pressure measurement P_{S1} will therefore be too low. The approximate operating points at which significant secondary separation was observed to occur, based on the mass flow measurements, are indicated on each of Figs. 11-15. This confluence point separation problem is similar to the plume-induced separation occurring in the base region of power-on missile flows.

It can also be seen in Figs. 11-15 that the experimentally measured maximum compression ratios are less than the values predicted by the simplified, one-dimensional theory. Based on P_{0P1}/P_{S1} values, the experimental ejector pressure recovery is 15-22% less than the theoretical values over the range of parameters investigated. Considering the simplicity of the one-dimensional model, an error of this magnitude is not surprising. Complex phenomena occurring in the mixing tube, such as primary/secondary mixing, boundary layer growth and separation, and shock wave/boundary layer/mixing layer interactions, have been ignored. These results do indicate, however, that if an empirical pressure recovery factor of roughly 0.8 is applied to the one-dimensional model, compression ratios within a few percent of the experimental values can be expected.

Axial wall pressure distributions were also obtained for each configuration investigated. Distributions for the $M_{P1}/M_{S1}=2.5/2.0$ ejector, corresponding to maximum compression conditions near the matched pressure point, upper limit point, and an intermediate operating point, are presented in Fig. 16. At the matched pressure point, the wall pressure is initially constant, then a monotonic increase occurs that then levels off to the exit value. At the upper limit point, the wall pressure exhibits an initial rise followed by a nearly linear increase to the exit. The initial pressure rise can

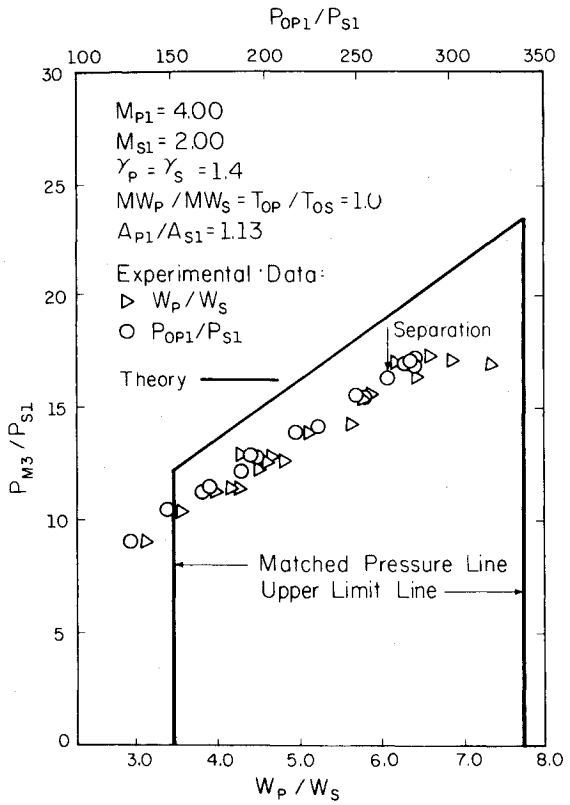

Fig. 15 Comparison of experimental and theoretical ejector compression characteristics, $M_{PI}/M_{SI} = 4.0/2.0$.

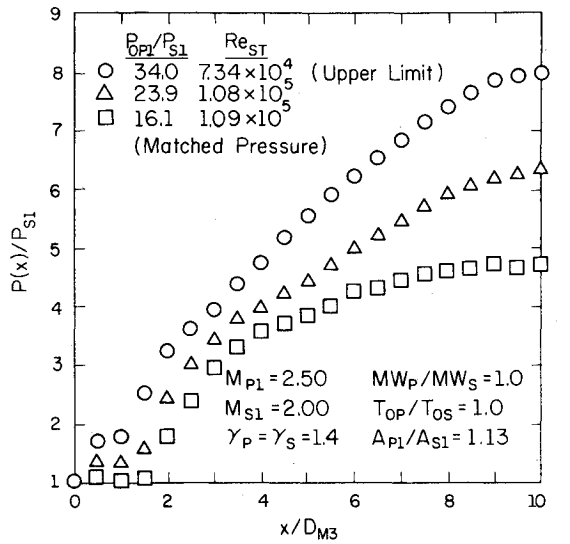

Fig. 16 Mixing tube wall pressure distributions for ejector at maximum compression conditions, $M_{PI}/M_{SI} = 2.5/2.0$.

be attributed to diffusion of the secondary stream as it is compressed by the primary stream in the initial interaction region.

At the upper limit point and the intermediate operating point in Fig. 16, it appears that the static pressure is still rising at the tube exit. Thus it appears that the mixing tube was not of sufficient length for the diffusion process to be completed. This, in turn, may explain some of the discrepancies between the theoretical predictions and experimental measurements of the compression ratio presented in Figs. 11-15. However, a further series of experiments was conducted for the $M_{PI}/M_{SI} = 2.5/2.0$ ejector with five mixing tube lengths:

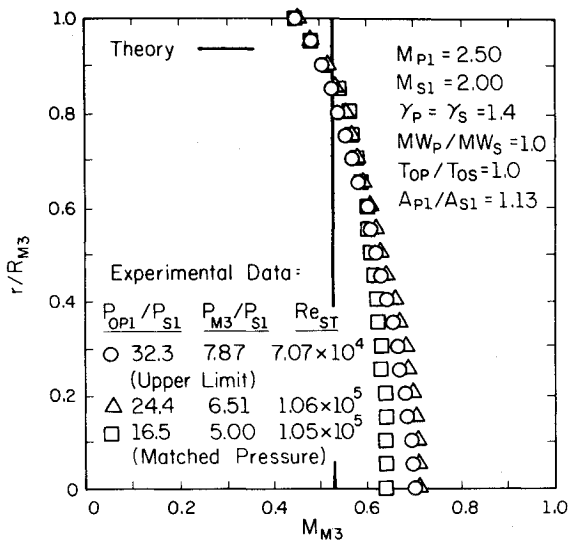

Fig. 17 Exit Mach number distributions for ejector at maximum compression conditions, $M_{PI}/M_{SI} = 2.5/2.0$.

$L/D = 5$, 7.5, 10, 12.5, and 15. These experiments demonstrated that the overall ejector performance was essentially identical for all configurations with $L/D \geq 7.5$. Only for the $L/D = 5$ mixing tube was the ejector performance significantly degraded because of the inadequate mixing and recompression length available.

For the same ejector and operating conditions similar to those presented in Fig. 16, the exit Mach number distributions were also measured. The results are presented in Fig. 17. These measurements demonstrate that the exit flow is reasonably well mixed and uniform, since distinct primary and secondary streams cannot be identified at the tube exit.

Conclusions

A theoretical and experimental investigation of the constant area, supersonic-supersonic ejector was conducted. A simplified theory based on one-dimensional models of the constant area mixing section and inviscid interaction region was developed to predict the pressure recovery performance of the device. The analysis identified seven variables of importance, and the parametric dependence of the compression ratio on each of these variables was presented. It was found that the dependence on the primary and secondary inlet Mach numbers and the primary-to-secondary molecular weight and stagnation temperature ratios is strong; therefore, ejector performance can be maximized by compression of the secondary stream and by use of a low molecular weight, high stagnation temperature, high Mach number primary gas.

A series of small-scale, axisymmetric experiments was conducted for five ejector configurations. These experiments indicated that, as the primary-to-secondary static pressure ratio at the mixing tube inlet is increased, separation of the secondary stream occurs, thus degrading ejector performance. Comparison of the measured and predicted compression ratios for the configurations studied suggested that application of an empirical factor of 0.8 to the one-dimensional theory will provide pressure recovery information of acceptable accuracy for engineering purposes.

Acknowledgment

This work was supported by the U.S. Army Research Office, Grant DAHC 04-75-G-0046; the U.S. Army Missile R&D Command, Research Contract DAAK 40-76-C-0942; and the Department of Mechanical and Industrial Engineering, University of Illinois at Urbana-Champaign.

References

[1]Mikkelsen, C. D., Sandberg, M. R., and Addy, A. L., "Theoretical and Experimental Analysis of the Constant-Area, Supersonic-Supersonic Ejector," Dept. of Mechanical and Industrial Engineering, Univ. of Illinois at Urbana-Champaign, Rept. UILU-ENG-76-4003, Oct. 1976.

[2]Spiegel, J. M., Hofstetter, R. V., and Kuehn, D. M., "Applications of Auxiliary Air Injectors to Supersonic Wind Tunnels," NACA RM A53I01, 1953.

[3]Hunczak, H. R. and Rousso, M. D., "Starting and Operating Limits of Two Supersonic Wind Tunnels Utilizing Auxiliary Air Injection," NACA TN 3262, 1954.

[4]Hasel, L. E. and Sinclair, A. R., "A Preliminary Investigation of Methods for Improving the Pressure-Recovery Characteristics of Variable-Geometry Supersonic-Subsonic Diffuser Systems," NACA RM L57H02, 1957.

[5]Stokes, G. M., "Description of a 2-Foot Hypersonic Facility at the Langley Research Center," NASA TN D-939, 1961.

[6]Zimet, E., "Steady State and Transient Operation of an Ejector for a Chemical Laser Cold Flow Mixing Experiment," Naval Surface Weapons Center/WOL/TR 76-142, Oct. 1976.

[7]Batt, R. G. and Behrens, H. W., "Chemical Laser Advanced Diffuser Ejector (CLADE) Program Alternate V—Far Advanced Technology Concepts," TRW Systems Group, Redondo Beach, Calif., DRCPM-HEL-CR-79-1, Oct. 1978.

[8]Fabri, J. and Paulon, J., "Theory and Experiments on Supersonic Air-to-Air Ejectors," NACA TM 1410, 1958.

[9]Fabri, J. and Siestrunck, R., "Supersonic Air Ejectors," *Advances in Applied Mechanics,* Vol. V, Academic Press, New York, 1958, pp. 1-34.

[10]Addy, A. L., "The Analysis of Supersonic Ejector Systems," *Supersonic Ejectors,* AGARDograph 163, 1972, pp. 31-101.

[11]Addy, A. L., "The Analysis of Supersonic Ejector Systems," *Ejectors,* von Kármán Institute, Lecture Series No. 79, Rhode Saint Genese, Belgium, 1975, pp. 1-41.

[12]Dutton, J. C. and Addy, A. L., "One-Dimensional Analyses of Supersonic-Supersonic Ejector-Diffuser Systems for Chemical Laser Applications," Dept. of Mechanical and Industrial Engineering, Univ. of Illinois at Urbana-Champaign, Rept. UILU-ENG-78-4015, Sept. 1978.